Heat Transfer—Asian Research, **42** (6), 2013

Mixed Convection Heat and Mass Transfer Over a Vertical Plate in a Power-Law Fluid-Saturated Porous Medium with Radiation and Chemical Reaction Effects

D. Srinivasacharya and G. Swamy Reddy
Department of Mathematics, National Institute of Technology, Warangal, A.P., India

Mixed convection heat and mass transfer from a vertical plate embedded in a power-law fluid-saturated Darcy porous medium with chemical reaction and radiation effects is studied. The governing partial differential equations are transformed into ordinary differential equations using similarity transformations and then solved numerically using the shooting method. A parametric study of the physical parameters involved in the problem is conducted and a representative set of numerical results is illustrated graphically. © 2013 Wiley Periodicals, Inc. Heat Trans Asian Res, 42(6): 485–499, 2013; Published online 1 April 2013 in Wiley Online Library (wileyonlinelibrary.com/journal/htj). DOI 10.1002/htj.21058

Key words: mixed convection, vertical plate, porous media, boundary layer, chemical reaction, radiation effects, power-law fluid, self-similarity

1. Introduction

The analysis of a mixed convection boundary layer flow along a vertical surface embedded in porous media has received considerable theoretical and practical interest. The mixed convection flow occurs in several industrial and technical applications such as electronic devices cooled by fans, nuclear reactors cooled during an emergency shutdown, a heat exchanger placed in a low-velocity environment, solar collectors, and so on. A number of studies have been reported in the literature focusing on the problem of mixed convection about different surface geometries in porous media. A review of convective heat transfer in porous medium is presented in the book by Nield and Bejan [1]. The majority of these studies dealt with the traditional Newtonian fluids. It is well known that most fluids which are encountered in chemical and allied processing applications do not satisfy the classical Newton's law and are accordingly known as non-Newtonian fluids. Due to the important applications of non-Newtonian fluids in biology, physiology, technology, and industry, considerable efforts have been directed towards the analysis and understanding of such fluids. A number of mathematical models have been proposed to explain the rheological behavior of non-Newtonian fluids. Among these, a model which has been most widely used for non-Newtonian fluids, and is frequently encountered in chemical engineering processes, is the power-law model. Although this model is merely an empirical relationship between the stress and velocity gradients, it has been successfully applied to non-Newtonian fluids experimentally.

The prediction of heat or mass transfer characteristics for mixed or natural convection of non-Newtonian fluids in porous media is very important due to its practical engineering applications, such as oil recovery and food processing. Abo-Eldahab and Salem [2] studied the problem of a laminar mixed convection flow of non-Newtonian power-law fluids from a constantly rotating isothermal cone or disk in the presence of a uniform magnetic field. Kumari and Nath [3] considered the conjugate mixed convection conduction heat transfer of a non-Newtonian power-law fluid on a vertical heated plate which is moving in an ambient fluid. Degan et al. [4] presented an analytical method to investigate transient free convection boundary layer flow along a vertical surface embedded in an anisotropic porous medium saturated by a non-Newtonian fluid. Chamkha and Al-Humoud [5] studied mixed convection heat and mass transfer of non-Newtonian fluids from a permeable surface embedded in a porous medium under a uniform surface temperature and concentration species. Chen [6] considered the problem of a magnetohydrodynamic mixed convective flow and heat transfer of an electrically conducting power-law fluid past a stretching surface in the presence of heat generation/absorption and thermal radiation. Elgazery and Abd Elazem [7] analyzed numerically a mathematical model to study the effects of a variable viscosity and thermal conductivity on unsteady heat and mass transfer in a non-Newtonian power-law fluid flow through a porous medium past a semi-infinite vertical plate with variable surface temperature in the presence of a magnetic field and radiation. Effects of double dispersion on mixed convection heat and mass transfer in a non-Newtonian fluid-saturated non-Darcy porous medium has been investigated by Kairi and Murthy [8]. Chamkha et al. [9] studied the effects of melting, thermal radiation, and heat generation or absorption on a steady mixed convection from a vertical wall embedded in a non-Newtonian power-law fluid-saturated non-Darcy porous medium for aiding and opposing external flows. Hayat et al. [10] investigated the magnetohydrodynamic (MHD) mixed convection stagnation-point flow and heat transfer of power-law fluids towards a stretching surface using the homotopy analysis method (HAM).

Radiation effects on convective heat transfer and MHD flow problems have assumed increasing importance in electrical power generation, astrophysical flows, solar power technology, space vehicle re-entry, and other industrial areas. Since the solution for convection and radiation equations is quite complicated, there are few studies about the simultaneous effect of convection and radiation for internal flows. Salem [11] has considered the coupled heat and mass transfer in Darcy–Forchheimer mixed convection from a vertical flat plate embedded in a fluid-saturated porous medium under the effects of radiation and viscous dissipation. Damseh [12] has studied magnetohydrodynamics-mixed convection from a radiated vertical isothermal surface embedded in a saturated porous media. The radiation effect on MHD mixed convection flow about a permeable vertical plate was studied by Orhan Aydn [13]. Hayat et al. [14] have considered the effects of radiation and magnetic field on the mixed convection stagnation-point flow over a vertical stretching sheet in a porous medium. Srinivasacharya et al. [15] studied the magnetic and radiation effects on mixed convection heat transfer along a vertical flat plate.

Chemical reaction effects on heat and mass transfer with radiation are of considerable importance in hydrometallurgical industries and chemical technology such as polymer production and food processing. Prabhu et al. [16] have considered the effects of chemical reaction, heat and mass transfer on MHD flow over a vertical stretching surface with a heat source, and thermal stratification effects. Postelnicu [17] studied the influence of chemical reaction on heat and mass transfer by natural convection from vertical surfaces in porous media by considering Soret and Dufour effects. Ibrahim et al. [18] analyzed the effects of chemical reaction and radiation absorption on the

unsteady MHD free convection flow past a semi-infinite vertical permeable moving plate with heat source and suction. Recently Dulal Pal and Hiranmoy Mondal [19] studied the influence of chemical reaction and thermal radiation on mixed convection heat and mass transfer over a stretching sheet in Darcy porous medium with Soret and Dufour effects.

Motivated by the investigations mentioned above, the aim of this investigation is to consider the effects of radiation and chemical reaction on the mixed convection heat and mass transfer along a vertical plate embedded in a power-law fluid-saturated porous medium. It is established that similarity solutions are possible only when the variation in the temperature and concentration are linear functions of the distance from the leading edge measured along the plate. Using these similarity transformations, the governing system of partial differential equations is transformed into a system of nonlinear ordinary differential equations and then solved numerically using a shooting method along with fourth-order Runge–Kutta integration.

Nomenclature

A: dimensional constant
B: dimensional constant
C_p: specific heat capacity
C_s: concentration susceptibility
C: concentration
C_w: wall concentration
C_∞: ambient concentration
D_m: mass diffusivity
N: buoyancy ratio
g: gravitational acceleration
K: Darcy permeability
k_T: thermal diffusion ratio
Le: Lewis number
Nu_x: local Nusselt number
n: power-law index
Sh_x: local Sherwood number
k: thermal conductivity
k_1: rate of chemical reaction
R: radiation parameter
Nu_x: local Nusselt number
T: temperature
T_w: wall temperature
T_∞: ambient temperature
u_∞: free stream velocity
u, v: velocity components in x and y directions
x, y: coordinates along and normal to the plate
q_y^r: radiative heat flux

Greek Symbols

α_m: thermal diffusivity
β_T, β_C: coefficients of thermal and solutal expansion
η: similarity variable
θ: dimensionless temperature
ϕ: dimensionless concentration
μ: dynamic viscosity
ν: kinematic viscosity
ρ: density of the fluid
ψ: stream function
σ^*: Stefan–Boltzmann constant

2. Mathematical Formulation

Consider a steady, laminar, incompressible, two-dimensional mixed convective heat and mass transfer along a vertical plate embedded in a free stream of non-Newtonian power-law fluid-saturated Darcy porous medium with velocity $U(x)$, temperature T_∞, and concentration C_∞. Choose the coordinate system such that the x-axis is along the vertical plate and the y-axis normal to the plate. The physical model and coordinate system are shown in Fig. 1. The plate is maintained at variable temperature and concentration, $T_w(x)$ and $C_w(x)$, respectively. These values are assumed to be greater than the ambient temperature T_∞ and concentration C_∞ at any arbitrary reference point in the medium (inside the boundary layer). Assume that the fluid and the porous medium have constant physical properties except for the density variation required by the Boussinesq approximation. The porous medium is isotropic and homogeneous. The fluid and the porous medium are in local thermodynamic equilibrium. The fluid is considered to be a gray, absorbing emitting radiation but non-scattering medium and the Rosseland approximation [20] is used to describe the radiative heat flux in the energy equation. The radiative heat flux in the x-direction is considered negligible in comparison to that in

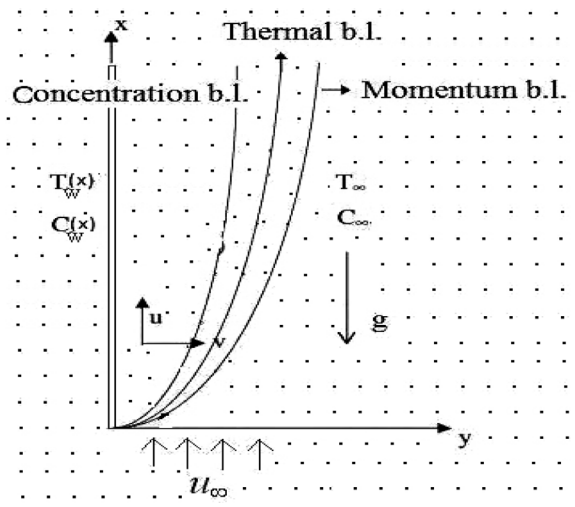

Fig. 1. Physical model and coordinate system.

the y-direction. Also, it is assumed that there exists a homogeneous chemical reaction of first-order with rate constant k_1 between the diffusing species and the fluid.

Using the Boussinesq and boundary layer approximations, the governing equations for the power-law fluid are given by

$$\frac{\partial u}{\partial x}+\frac{\partial v}{\partial y}=0 \tag{1}$$

$$u^n=\{U(x)\}^n+\frac{gK}{\upsilon}\left(\beta_T\left(T-T_\infty\right)+\beta_C\left(C-C_\infty\right)\right) \tag{2}$$

$$u\frac{\partial T}{\partial x}+v\frac{\partial T}{\partial y}=\frac{\partial}{\partial y}\left(\alpha_m\frac{\partial T}{\partial y}-\frac{1}{\rho C_P}q_y{}^r\right) \tag{3}$$

$$u\frac{\partial C}{\partial x}+v\frac{\partial C}{\partial y}=D_m\frac{\partial^2 C}{\partial y^2}+k_1(C-C_\infty) \tag{4}$$

where u and v are the Darcian velocity components along x and y directions, T is the temperature, C is the concentration, k_T is the thermal diffusion ratio, ν is the kinematic viscosity, K is the permeability, g is the acceleration due to gravity, β_T is the coefficient of thermal expansion, β_C is the coefficient of concentration expansion, α_m is the thermal diffusivity, D_m is the mass diffusivity of the porous medium, C_p is the specific heat capacity, C_s is the concentration susceptibility, k_1 is the rate of chemical reaction, q_y^r is the radiative heat flux term, and n is the power-law index. When $n = 1$, Eq. (2) represents a Newtonian fluid. Therefore, deviation of n from unity indicates the degree of deviation from Newtonian behavior. For $n < 1$, the fluid is shear thinning and for $n > 1$, the fluid is shear thickening.

The boundary conditions are

$$v=0,\quad T=T_w(\mathrm{x}),\quad C=C_w(\mathrm{x})\qquad \text{at}\qquad y=0 \tag{5a}$$

$$u\to U(x),\quad T\to T_\infty,\quad C\to C_\infty\qquad \text{as}\qquad y\to\infty \tag{5b}$$

where the subscripts w and ∞ indicate the conditions at the wall and at the outer edge of the boundary layer, respectively.

The radiative heat flux q_y^r is described by the Rosseland approximation such that

$$q_r=-\frac{4\sigma^*}{3k^*}\frac{\partial T^4}{\partial y} \tag{6}$$

where σ^* and k^* are the Stefan–Boltzmann constant and the mean absorption coefficient, respectively. We assume that the differences of the temperature within the flow are sufficiently small such that T^4 may be expressed as a linear function of the temperature. This is accomplished by expanding in a Taylor series about T_∞ and neglecting higher-order terms, thus

$$T^4=4T_\infty^3T-3T_\infty^4 \tag{7}$$

In view of the continuity Eq. (1), we introduce the stream function ψ by

$$u = \frac{\partial \psi}{\partial y}, \quad v = -\frac{\partial \psi}{\partial x} \tag{8}$$

Substituting Eq. (8) in Eqs. (2) to (4) and then using the following similarity transformations

$$\left.\begin{aligned} &\eta = B\,y, \quad \psi = Axf(\eta), \\ &\theta(\eta) = \frac{T - T_\infty}{T_w(x) - T_\infty}, \; T_w(x) - T_\infty = E\,x^n \\ &\phi(\eta) = \frac{C - C_\infty}{C_w(x) - C_\infty}, \; C_w(x) - C_\infty = F\,x^n \end{aligned}\right\} \tag{9}$$

we get the following nonlinear system of differential equations.

$$(f')^n = (1 + \theta + \mathrm{N}\phi) \tag{10}$$

$$\left(1 + \frac{4}{3}R\right)\theta'' = (n\,f'\theta - f\theta') \tag{11}$$

$$\phi'' = Le(n f'\phi - f\phi' + \gamma\phi) \tag{12}$$

where primes denote differentiation with respect to η alone, $R = 4\sigma^* T_\infty^3/k^* k$ is the conduction radiation parameter, $\gamma = k_1/B^2\alpha_m$ is the chemical reaction parameter, $N = \beta_C(C_w - C_\infty)/\beta_T(T_w - T_\infty)$ is the buoyancy ratio, $Le = \alpha_m/D_m$ is the Lewis number, $A = (EgK\beta_T\alpha_m^n/\nu)^{1/2n}$, and $B = (EgK\beta_T/\nu\alpha_m^n)^{1/2n}$.

The boundary conditions (5) in terms of f, θ, and φ become

$$f(0) = 0, \quad \theta(0) = 1, \quad \phi(0) = 1, \; f'(\infty) = 1, \; \theta(\infty) = 0, \; \phi(\infty) = 0 \tag{13}$$

The parameters of engineering interest for the present problem are the Nusselt and Sherwood numbers, which are given by the expressions

$$\frac{Nu_x}{Bx} = -\theta'(0) \quad \text{and} \quad \frac{Sh_x}{Bx} = -\phi'(0) \tag{14}$$

The flow Eq. (10) and the energy and concentration Eqs. (11) and (12) constitute a set of nonlinear non-homogeneous differential equations for which closed-form solution cannot be obtained. Hence the problem is numerically using a shooting technique along with fourth-order Runge–Kutta integration. The nonlinear differential Eqs. (10) to (12) are converted into the system of first-order linear differential equations and then integrated using the fourth-order Runge–Kutta method from $\eta = 0$ to $\eta = \eta_{max}$ over successive steps $\Delta\eta$ by giving appropriate initial guess values for $f^1(0)$, $\theta^1(0)$, and $\phi^1(0)$ as they are not specified in Eq. (13). Here η_{max} is the value of η at ∞ and is chosen large enough so that the solution shows little further change for η larger than η_{max}. The accuracy of the assumed initial values $f^1(0)$, $\theta^1(0)$, and $\phi^1(0)$ is then checked by comparing the calculated values of $f^1(0)$, $\theta^1(0)$, and $\phi^1(0)$ at $\eta = \eta_{max}$ with their given value in Eq. (13). If a difference exists, another set of initial values for $f^1(0)$, $\theta^1(0)$, and $\phi^1(0)$ are assumed and the process is repeated until the agreement between the calculated and the given condition at $\eta = \eta_{max}$ is within the specified

degree of accuracy. In order to see the effects of step size ($\Delta\eta$) we ran the code for our model with three different step sizes as $\Delta\eta = 0{:}01$, $\Delta\eta = 0{:}001$, and $\Delta\eta = 0{:}005$ and in each case we found very good agreement between them. A step size of $\Delta\eta = 0{:}01$ is selected to be satisfactory for a convergence criterion of 10^{-6} in all cases. In the present study, the boundary condition for η at ∞ varies with parameter values and it is suitably chosen at each time such that the velocity, temperature and concentration approach zero at the outer edge of the boundary layer. Extensive calculations are performed to obtain the wall velocity, temperature, and concentration fields for a wide range of parameters.

3. Results and Discussion

The non-dimensional velocity $f'(\eta)$, temperature $\theta(\eta)$, and concentration $\phi(\eta)$ are plotted for $N = 1$, $Le = 1$, $\gamma = 0.5$ in Figs. 2 to 4 with varying radiation parameters by considering pseudo-plastic fluids with $n = 0.5$. Figure 2 demonstrates that the velocity of the fluid increased with the increase in the value of the radiation parameter. It can be noted from Fig. 3 that the temperature of the fluid increased with the increase in the value of the radiation parameter. It can be found from Fig. 4 that the concentration of the fluid is decreased with an increase in the value of the radiation parameter. These results can be explained by the fact that an increase in the radiation parameter $R = 4\sigma^* T_\infty^3 / k^* k$ for given k and T_∞ means a decrease in the Rosseland radiation absorptivity k^*. Hence, the divergence of radiative heat flux q_r increases as k^* decreases. Therefore, the rate of radiative heat transferred to the fluid increases and consequently the fluid temperature along with the velocity of its particle also increases.

The variation of the non-dimensional velocity $f'(\eta)$, temperature $\theta(\eta)$, and concentration $\phi(\eta)$ are plotted for $N = 1$, $Le = 1$, $\gamma = 0.5$ with a varying radiation parameter by considering Newtonian fluids with $n = 1$ as shown in Figs. 5 to 7. It can be observed from Figs. 5 and 6 that the velocity and temperature of the fluid increased with an increase in the value of the radiation parameter. It can be seen from Fig. 7 that the concentration of the fluid is decreased by increasing the value of the radiation

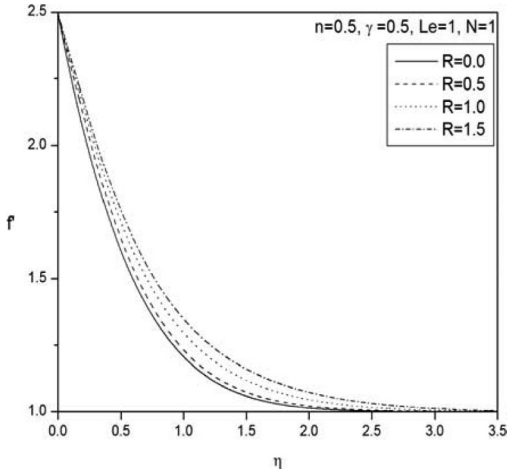

Fig. 2. Velocity profiles for various values of R for pseudo-plastic fluids.

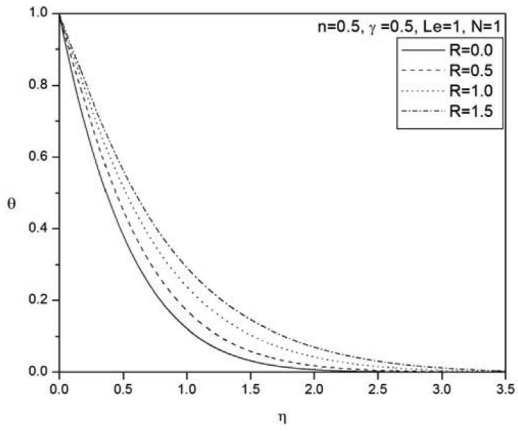

Fig. 3. Temperature profiles for various values of R for pseudo-plastic fluids.

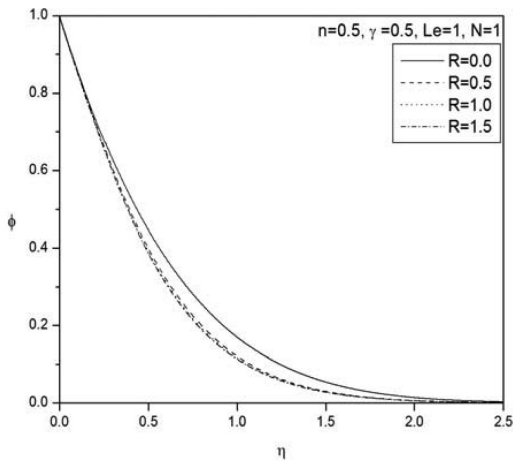

Fig. 4. Concentration profiles for various values of *R* for pseudo-plastic fluids.

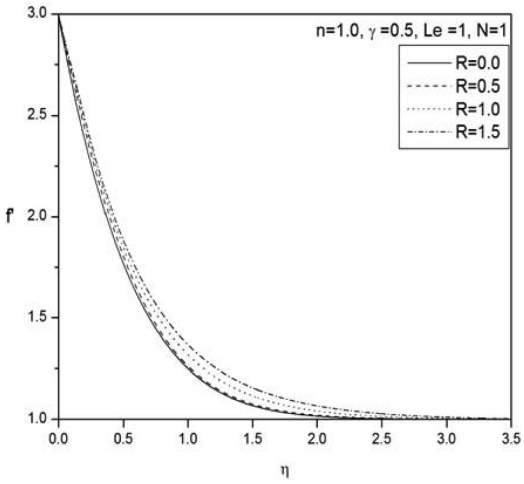

Fig. 5. Velocity profiles for various values of *R* for Newtonian fluid.

parameter. Increasing the thermal radiation parameter produces an increase in the thermal condition of the fluid and its thermal boundary layer. More flow is induced in the boundary layer by the increase in the fluid temperature thereby causing the velocity of the fluid to increase as well.

The effect of the radiation parameter on the non-dimensional velocity $f'(\eta)$, temperature $\theta(\eta)$, and concentration for $N = 1$, $Le = 1$, $\gamma = 0.5$ is depicted in Figs. 8 to 10 in the presence of dilatant fluids with $n = 1.5$. From Fig. 8 it is noticed that the velocity of the fluid increased with an increase in the value of the radiation parameter. Figure 9 demonstrates that the temperature fluid increased with an increase in the value of the radiation parameter. This result qualitatively agrees with

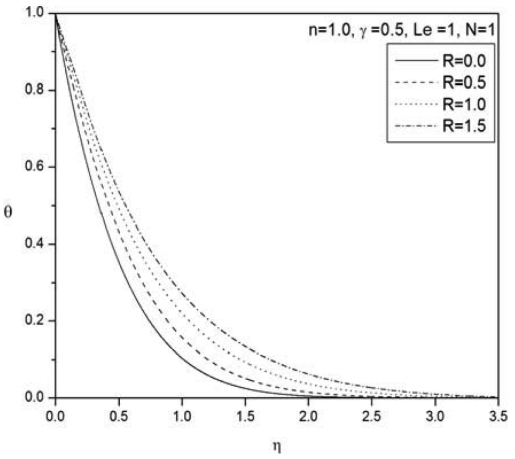

Fig. 6. Temperature profiles for various values of *R* for Newtonian fluid.

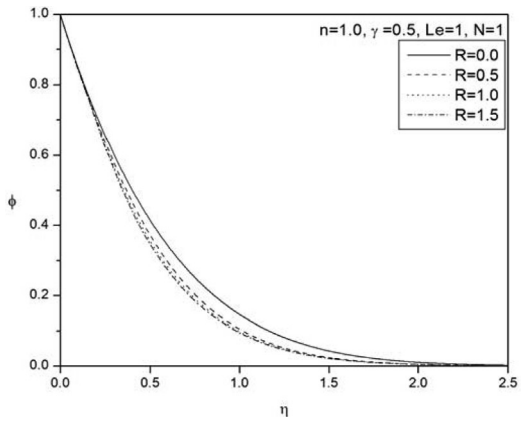

Fig. 7. Concentration profiles for various values of *R* for Newtonian fluid.

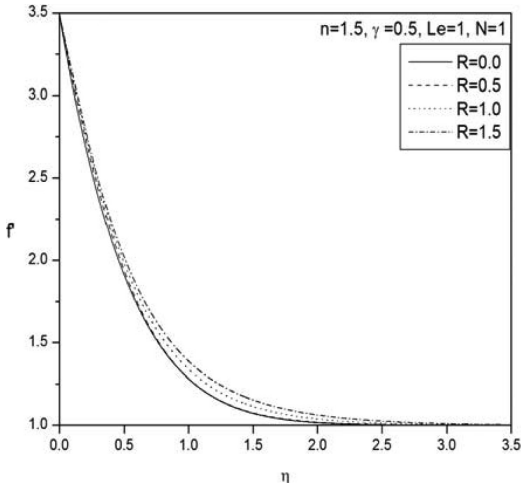

Fig. 8. Velocity profiles for various values of R for dilatant fluids.

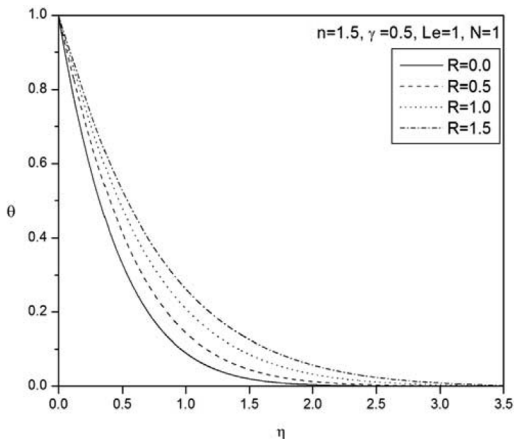

Fig. 9. Temperature profiles for various values of R for dilatant fluids.

expectations since the effects of radiation and surface temperature are to increase the rates of energy transport to the fluid, thus increasing the temperature of the fluid. Figure 10 illustrates that the concentration of the fluid is decreased by increasing the value of the radiation parameter. The presence of thermal radiation enhances the thermal state of the fluid causing its temperature to increase and the solute concentration to decrease.

The non-dimensional velocity $f'(\eta)$, temperature $\theta(\eta)$, and concentration $\phi(\eta)$ are plotted for $N = 1$, $Le = 1$, $R = 0.5$ in Figs. 11 to 13 with varying the chemical reaction parameter by considering pseudo-plastic fluids with $n = 0.5$. It can be observed from Fig. 11 that the velocity of the fluid decreases with an increase in the value of the chemical reaction parameter. Figure 12 demonstrates that the temperature of the fluid increased with the increasing value of the chemical reaction parameter.

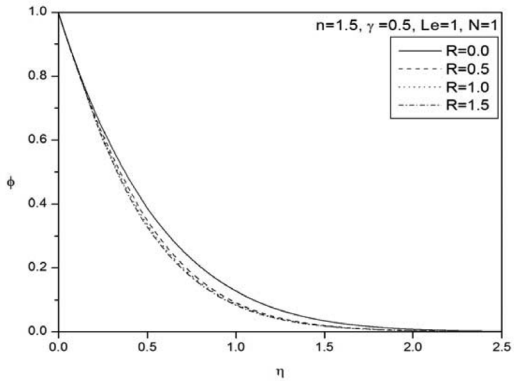

Fig. 10. Concentration profiles for various values of R for dilatant fluids.

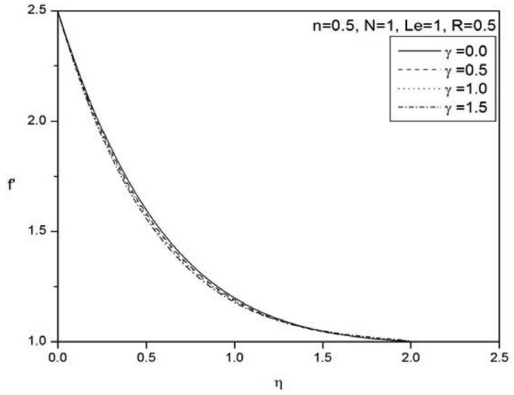

Fig. 11. Velocity profiles for various values of γ for pseudo-plastic fluids.

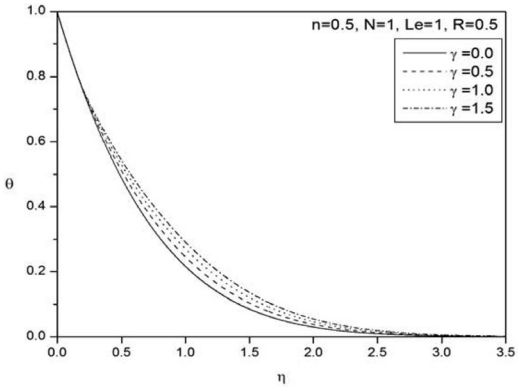

Fig. 12. Temperature profiles for various values of γ for pseudo-plastic fluids.

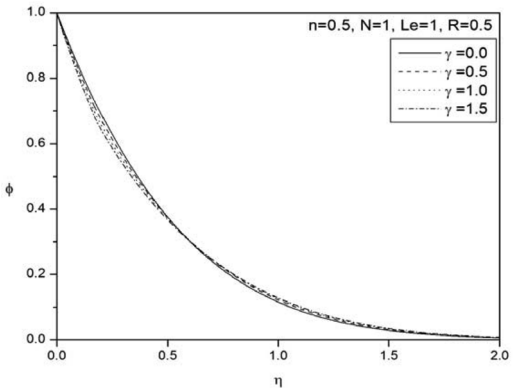

Fig. 13. Concentration profiles for various values of γ for pseudo-plastic fluids.

It is clear from Fig. 13 that the concentration of the fluid is decreased with an increase in the value of the chemical reaction parameter. Higher values of γ amount to a fall in the chemical molecular diffusivity, i.e., less diffusion. Therefore, they are obtained by species transfer. An increase in γ will suppress species concentration. The concentration distribution decreases at all points of the flow field with the increase in the reaction parameter.

The variation of the non-dimensional velocity $f'(\eta)$, temperature $\theta(\eta)$, and concentration $\phi(\eta)$ are plotted for $N = 1$, $Le = 1$, $R = 0.5$ with a varying chemical reaction parameter by considering Newtonian fluids with $n = 1.0$ as shown in Figs. 14 to 16. Figure 14 illustrates that the velocity of the fluid decreases with an increase in the value of the chemical reaction parameter. It can be found from Fig. 15 that the temperature of the fluid increased with the increasing value of the chemical reaction parameter. Figure 16 demonstrates that the increase in the value of the chemical reaction parameter decreases the concentration of the fluid in the medium.

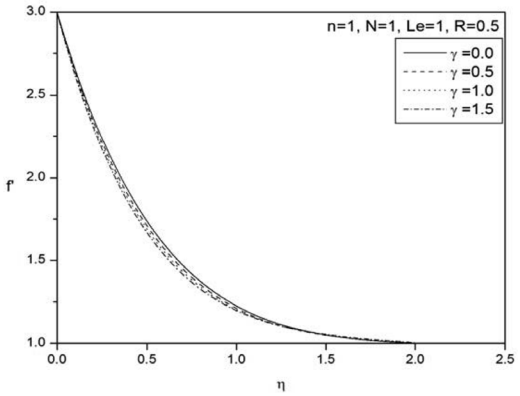

Fig. 14. Velocity profiles for various values of γ for Newtonian fluid.

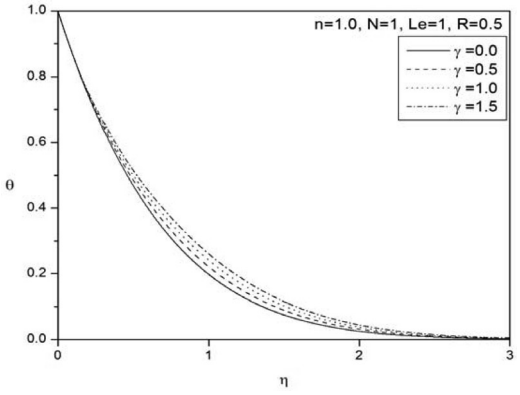

Fig. 15. Temperature profiles for various values of γ for Newtonian fluid.

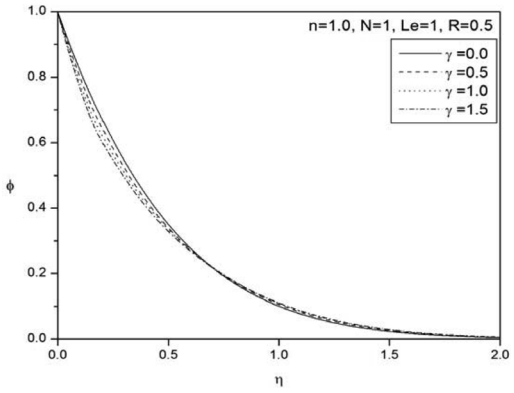

Fig. 16. Concentration profiles for various values of γ for Newtonian fluid.

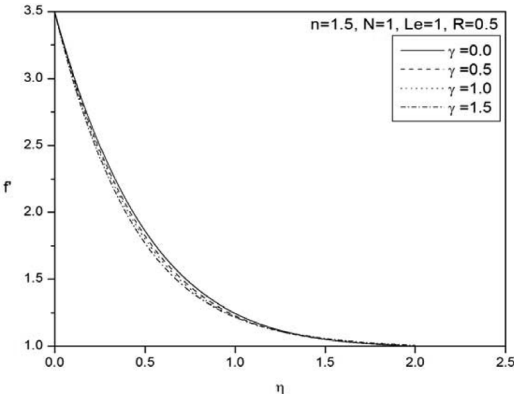

Fig. 17. Velocity profiles for various values of γ for dilatant fluids.

In Figs. 17 to 19, the effects of the chemical reaction parameter on the dimensionless velocity, temperature, and concentration are presented for fixed values of $N = 1$, $Le = 1$, $R = 0.5$ in the presence of dilatant fluids with $n = 1.5$. It is observed from Fig. 17 that the velocity of the fluid decreases with an increase in the value of the chemical reaction parameter. It can be observed from Fig. 18 that the temperature of the fluid increased with an increase in the value of the chemical reaction parameter. Figure 19 illustrates that the concentration of the fluid is decreased by increasing the value of the chemical reaction parameter.

The non-dimensional velocity $f'(\eta)$, temperature $\theta(\eta)$, and concentration $\phi(\eta)$ for $N = 1$, $Le = 1.5$, $\gamma = 0.5$, $R = 0.5$ with a variation in the power-law index parameter is plotted in Figs. 20 to 22. It is found from Fig. 20 that the fluid velocity is increased with an increase in the value of the power-law index parameter. The effect of the increasing values of the power-law index n is to increase the horizontal boundary layer thickness. That is, the thickness is much smaller for shear thinning (pseudo-

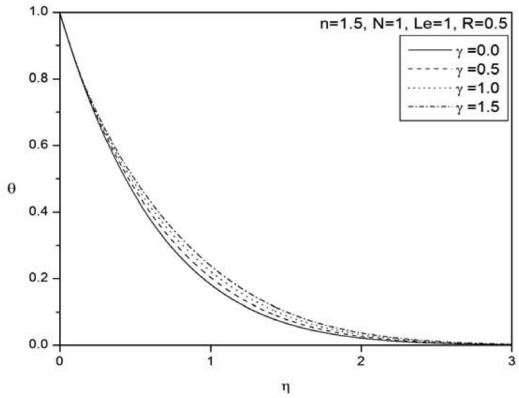

Fig. 18. Temperature profiles for various values of γ for dilatant fluids.

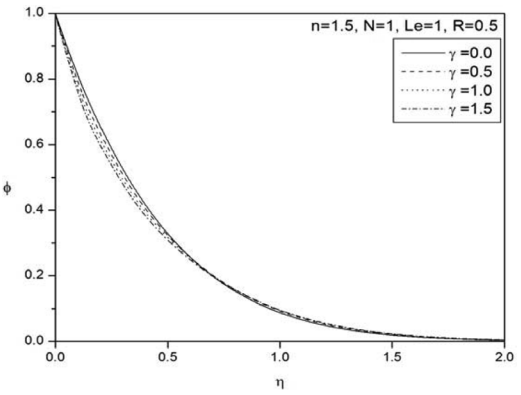

Fig. 19. Concentration profiles for various values of γ for dilatant fluids.

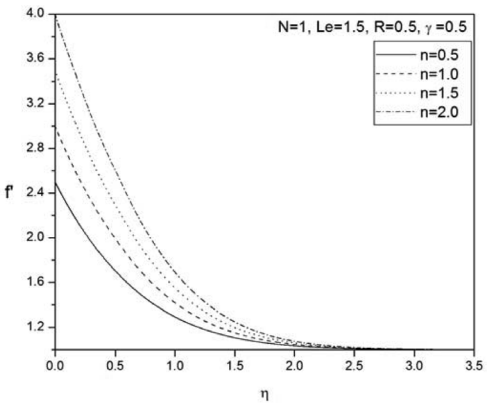

Fig. 20. Velocity profiles for various values of power-law index (n).

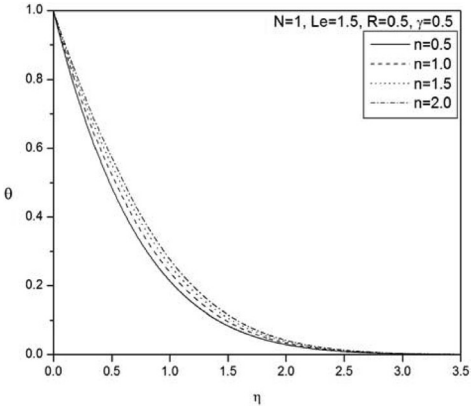

Fig. 21. Temperature profiles for various values of power-law index (n).

plastic; $n < 1$) fluids than that of shear thickening (dilatants; $n > 1$) fluids. In the case of a shear thinning fluid ($n < 1$), the shear rates near the walls are higher than those for a Newtonian fluid. It can be seen from Figs. 21 and 22 the temperature and concentration in the fluid is increased with an increase in the value of the power-law index (n). Increasing the values of the power-law index (n) tends to accelerate the flow and increase the thermal and solutal boundary layer thickness.

Table 1 shows the effects of n, Le, R, γ, and N on the non-dimensional heat and mass transfer coefficients. It is seen from this table that both the heat and mass transfer rates increase with increasing power-law index n. The Lewis number (diffusion ratio) is the ratio of the Schmidt number (ν/D_m) and Prandtl number (ν/α_m). As the Lewis number increases, i.e., Schmidt number increases (or Prandtl number decreases), the Nusselt number is decreasing while the Sherwood number is increasing. The Schmidt number quantifies the relative effectiveness of momentum and mass transport by diffusion in the hydrodynamic (velocity) and concentration (species) boundary layers. Hence the rate of mass transfer is increased with the increase in Schmidt number or Lewis number. Similarly, a

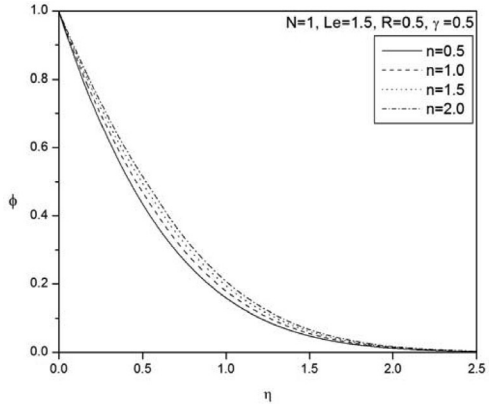

Fig. 22. Concentration profiles for various values of power-law index (n).

Table 1. Variation of Nondimensional Heat and Mass Transfer Coefficients for Various Values of n, Le, R, γ, and N

n	Le	R	γ	N	$-\theta'(0)$	$-\phi'(0)$
0.0	1.0	0.5	0.5	1.0	1.245490	1.365690
0.5	1.0	0.5	0.5	1.0	1.356002	1.518363
1.0	1.0	0.5	0.5	1.0	1.456792	1.658001
1.5	1.0	0.5	0.5	1.0	1.550090	1.787529
2.0	1.0	0.5	0.5	1.0	1.637377	1.908908
1.5	0.0	0.5	0.5	1.0	1.698012	0.200000
1.5	0.5	0.5	0.5	1.0	1.589839	1.290289
1.5	1.0	0.5	0.5	1.0	1.550090	1.787529
1.5	1.5	0.5	0.5	1.0	1.525437	2.144739
1.5	2.0	0.5	0.5	1.0	1.507894	2.429258
1.5	1.0	0.0	0.5	1.0	2.015786	2.146391
1.5	1.0	0.5	0.5	1.0	1.527149	2.170578
1.5	1.0	1.0	0.5	1.0	1.270887	2.184633
1.5	1.0	1.5	0.5	1.0	1.108015	2.194066
1.5	1.0	2.0	0.5	1.0	0.993519	2.200927
1.5	1.0	0.5	0.0	1.0	1.533632	2.050555
1.5	1.0	0.5	0.5	1.0	1.527149	2.170578
1.5	1.0	0.5	1.0	1.0	1.521233	2.284290
1.5	1.0	0.5	1.5	1.0	1.515800	2.392562
1.5	1.0	0.5	2.0	1.0	1.510779	2.496089
1.5	1.0	0.5	0.5	0.5	2.091634	2.574475
1.5	1.0	0.5	0.5	0.6	1.854253	2.228113
1.5	1.0	0.5	0.5	0.7	1.718388	2.031201
1.5	1.0	0.5	0.5	0.8	1.635401	1.911282
1.5	1.0	0.5	0.5	0.9	1.583134	1.835650
1.5	1.0	0.5	0.5	1.0	1.550107	1.787527

decrease in Prandtl number, i.e., increase in Lewis number, is equivalent to increasing the thermal conductivities, and therefore heat is able to diffuse away from the heated plate more rapidly. Hence the rate of heat transfer is reduced. The heat transfer rate is decreasing for increasing values of radiation parameter but the mass transfer rate is increasing. The chemical reaction parameter decreases the heat transfer coefficient but increases the mass transfer rate. Increase in the values of γ implies more interaction of species concentration with the momentum boundary layer and less interaction with the thermal boundary layer. Hence, the chemical reaction parameter has a more significant effect on the Sherwood number than it does on the Nusselt number. There is an increase in both the heat and mass transfer rates with an increase in the buoyancy ratio.

4. Conclusions

In this paper, mixed convection heat and mass transfer along a vertical plate embedded in a power-law fluid-saturated Darcy porous medium in the presence of radiation and chemical reaction has been considered. The wall is maintained at a variable temperature and concentration $T_w(x)$ and $C_w(x)$, respectively. It can be concluded from the present analysis that the higher values of the radiation parameter result in higher velocity and temperature distributions but concentration is decreased. An increase in the value of the chemical reaction parameter results in lower velocity and concentration distributions but higher temperature distribution. Also, the higher values of the power-law index parameter result in higher velocity, temperature, and concentration distributions within the boundary layer.

Literature Cited

1. Nield DA, Bejan A. Convection heat transfer. John Wiley; 1994.
2. Abo-Eldahab EM, Salem AM. MHD combined convection flow of a non-Newtonian power-law fluid due to a rotating cone or disk. Canadian J Phys 2004;82:531–540.
3. Kumari M, Nath G. Conjugate mixed convection transport from a moving vertical plate in a non-Newtonian. Fluid Int J Therm Sci 2006;45:607–614.
4. Degan G, Akowanou C, Awanou NC. Transient natural convection of non-Newtonian fluids about a vertical surface embedded in an anisotropic porous medium. Int J Heat Mass Transf 2007;50:4629–4639.
5. Chamkha AJ, Al-Humoud J. Mixed convection heat and mass transfer of non-Newtonian fluids from a permeable surface embedded in a porous medium. Int J Numer Meth Heat Fluid Flow 2007;17:195–212.
6. Chen CH. Magneto-hydrodynamic mixed convection of a power-law fluid past a stretching surface in the presence of thermal radiation and internal heat generation/absorption. Int J Non-Linear Mech 2009;44:596–603.
7. Elgazery NS, Abd Elazam NY. Effects of variable properties on magnetohydrodynamics unsteady mixed convection in non-Newtonian fluid with variable surface temperature. J Porous Media 2009;12:477–488.
8. Kairi RR, Murthy PVSN. Effect of double dispersion on mixed convection heat and mass transfer in a non Newtonian fluid-saturated non-Darcy porous medium. J Porous Media 2010;13:749–757.
9. Chamkha AJ, Sameh E, Ahmed, Abdulkareem S, Aloraier. Melting and radiation effects on mixed convection from a vertical surface embedded in a non-Newtonian fluid saturated non-Darcy porous medium for aiding and opposing eternal flows. Int J Phy Sci 2010;5:1212–1224.
10. Hayat T, Mustafa M, Obaidat S. Simultaneous effects of MHD and thermal radiation on the mixed convection stagnation-point flow of a power-law fluid. Chinese Phys Lett 2011;28:074702.
11. Salem AM. Coupled heat and mass transfer in Darcy-Forchheimer mixed convection from a vertical flat plate embedded in a fluid-saturated porous medium under the effects of radiation and viscous dissipation. J Korean Phys Soc 2006;48:409–413.
12. Damseh RA. Magneto hydrodynamics-mixed convection from radiate vertical isothermal surface embedded in a saturated porous media. Trans ASME 2006;73.
13. Orhan Aydn AK. Radiation effect on MHD mixed convection flow about a permeable vertical plate. Heat Mass Transf 2008;45:239–246.
14. Hayat T, Abbas Z, Pop I, Asghar S. Effects of radiation and magnetic field on the mixed convection stagnation-point flow over a vertical stretching sheet in a porous medium. Int J Heat Mass Transf 2010;53:466–474.
15. Srinivasacharya D, Pranitha J, RamReddy Ch. MHD and radiation effects on non-Darcy mixed convection. Int J Nonlinear Sci 2010;10(1):61–69.
16. Prabhu KKS, Kandasamy R, Periasamy K. Chemical reaction, heat and mass transfer on MHD flow over a vertical stretching surface with heat source and thermal stratification effects. Int J Heat Mass Transf 2005;48:4557–4561.
17. Postelnicu A. Influence of chemical reaction on heat and mass transfer by natural convection from vertical surfaces in porous media considering Soret and Dufour effects. Heat Mass Transf 2007;43:595–602.

18. Ibrahim FS, Elaiw AM, Bakr AA. Effect of the chemical reaction and radiation absorption on the unsteady MHD free convection flow past a semi infinite vertical permeable moving plate with heat source and suction. Nonlinear Sci Numer Simulat 2008;13:1056–1066.
19. Pal D, Mondal H. Influence of chemical reaction and thermal radiation on mixed convection heat and mass transfer over a stretching sheet in Darcy porous medium with Soret and Dufour effects. Energy Conversion Management 2012;62:102–108.
20. Sparrow EM, Cess RD. Radiation heat transfer. Hemisphere Publication; 1978.